

VLBI polarization observations of the rapidly variable BL Lacertae object BL 0716+714

D.C. Gabuzda¹, Y.Y. Kovalev^{1,2}, T.P. Krichbaum³, W. Alef³, A. Kraus³, A. Witzel³, and A. Quirrenbach⁴

¹ Astro Space Centre, Lebedev Physical Institute, Leninsky Pr. 53, 117924 Moscow, Russia

² Sternberg Astronomical Institute, Moscow State University, 13 Universitetsky Pr., 119899 Moscow, Russia

³ Max-Planck-Institut für Radioastronomie, Auf dem Hügel 69, D-53121 Bonn, Germany

⁴ Max-Planck-Institut für Extraterrestrische Physik, Giessenbachstrasse, Postfach 1603, D-85470 Garching bei München, Germany

Received 20 October 1997 / Accepted 6 January 1998

Abstract. New polarization-sensitive global VLBI and VLBA images of the BL Lacertae object BL 0716+714 at 6 cm (1991.43) and 3.6 cm/1.3 cm (1994.22) are presented. The source shows a compact, one-sided core–jet structure in structural position angle $\sim 13^\circ$. Comparison with previously published data suggests that the apparent velocity of a 6 cm jet component is $> 0.82 \pm 0.11c$, if the redshift of BL 0716+714 is $z > 0.3$ ($H_0 = 100 \text{ km s}^{-1} \text{ Mpc}^{-1}$; $q_0 = 0.5$). Linear polarization from the VLBI core was detected at all three frequencies. In addition, polarization from the innermost jet component was detected at 1.3 cm. This compact jet polarization is quite high, $\sim 50\%$, and is aligned with the jet direction, suggesting it is a transverse shock. The VLBI core polarization at our earlier epoch was perpendicular to the VLBI jet direction, but aligned with the jet direction at the later epoch, about three years later. The available evidence suggests that the very rapid variability that is sometimes observed in BL 0716+714 occurs on more compact scales than those imaged by our VLB array.

Key words: BL Lacertae objects: individual: BL 0716+714 – galaxies: jets – radio continuum: galaxies – polarization

1. Introduction

BL Lacertae objects are extragalactic sources displaying weak or undetectable line emission and strong and variable polarization in wavebands ranging from optical through radio. They typically have compact, flat-spectrum radio structure, and point-like optical structure (Angel and Stockman 1980; Kollgaard 1994). The radio emission and much of the optical emission is believed to be synchrotron radiation.

The polarization position angles χ in knots in the VLBI jets of BL Lacertae objects show a tendency to be parallel to the VLBI structural axis. The degrees of polarization in jet components have been observed to be as high as $m \sim 60 - 70\%$, with typical values $m \sim 5 - 15\%$, indicating that these components are optically thin and that in at least some cases the magnetic

field is very highly ordered. The inferred typical magnetic field direction is perpendicular to the jet direction, suggesting that the jet components are often associated with relativistic shocks that enhance the magnetic field transverse to the compression in the direction of propagation (Laing 1980; Hughes, Aller, & Aller 1989). The distribution of 6 cm core polarization orientations for BL Lacertae objects is bimodal, suggesting that χ_{core} is roughly perpendicular to the jet direction when the cores are quiescent, and aligns with the jet direction at epochs when the strong polarization from newly emerging shock components is blended with the core polarization (Gabuzda et al. 1994).

BL 0716+714 is one of a growing number of compact radio sources found to exhibit “intraday” variability on timescales less than or of the order of a day (IDV) (Heeschen et al. 1987; Wagner et al. 1996). It offers perhaps the best case for simultaneous IDV at optical and radio wavelengths (Quirrenbach et al. 1991). The optical spectrum of BL 0716+714 is featureless, and no redshift is known for this object. Based on the lack of detection of a host galaxy (see Wagner et al. 1996), the redshift is estimated to be $z > 0.3$. The 6 cm arcsecond-scale radio emission of this object has an amorphous double-lobed structure in position angle $\sim -55^\circ$ (Perley 1982; Wagner et al. 1996). BL 0716+714 is one of six BL Lacertae objects included in a small, but complete and homogeneous sample of thirteen flat-spectrum, high-declination sources. The milliarcsecond-scale structure probed by VLBI is very compact, with a dominant core and a jet directed almost directly to the north (Eckart et al. 1987; Witzel et al. 1988). The observations we present here indicate the presence of modestly superluminal and possibly even subluminal motion in the VLBI jet, and show that the parsec-scale polarization properties of this source are typical of those for BL Lacertae objects.

We assume throughout a Friedmann universe with Hubble constant of $100h \text{ km sec}^{-1} \text{ Mpc}^{-1}$ and $q_0 = 0.5$.

2. Observations

Our first (6 cm) observing epoch was 1991.43 (10:00 UT June 6 – 10:00 UT June 7), with a global array of ten antennas (Onsala 26 m, Medicina 32 m, Effelsberg 100 m, Jodrell Bank 26 m,

Table 1. Integrated polarization measurements

Telescope	Date	Wavelength (cm)	I (Jy)	p (mJy)	χ (deg)
0954+658 (calibrator)					
Michigan	94.03.20	3.6	0.91 ± 0.08	89 ± 47	-7 ± 22
Michigan	94.03.22	2.0	0.77 ± 0.02	55 ± 17	-22 ± 8
Effelsberg	94.03.20	2.8	0.63 ± 0.01	36 ± 1	-15.3 ± 1.0
Effelsberg	94.03.20	0.9	0.71 ± 0.01	31 ± 2	-16.6 ± 5.8
BL 0716+714					
Michigan	94.03.23	3.6	0.44 ± 0.10	80 ± 53	28 ± 15
Michigan	94.03.21	2.0	0.49 ± 0.02	18 ± 13	18 ± 21
Effelsberg	94.03.20	2.8	0.472 ± 0.008	9 ± 3	14 ± 8
Effelsberg	94.03.20	0.9	0.40 ± 0.01	7 ± 2	45 ± 11

Haystack 37 m, Green Bank 43 m, Los Alamos 25 m, Phased VLA $\sqrt{27} \times 25$ m, Pietown 25 m, and Owens Valley 25 m). The observations were made under the auspices of the US and European VLBI networks. The data were recorded using the MkIII system in dual polarization mode C, and all data were subsequently correlated using the Mk IIIA correlator at Haystack Observatory. About 35 6.5-minute observations of BL 0716+714 were made, spread over the entire time BL 0716+714 was observable with eight or more antennas.

Our second (3.6/1.3 cm) observing epoch was 1994.22 (6:00–24:00 UT March 21), using the ten VLBA antennas. These data were recorded using the VLBA system in MkIII dual polarization mode A and were correlated at Bonn. Thirty observations of BL 0716+714 were made at both 3.6 cm (5 minutes per scan) and 1.3 cm (8 minutes per scan), spread over the entire time BL 0716+714 was visible with eight or more antennas. In all cases, the u - v coverage, although not strictly continuous, was quite good, and no significant holes were introduced by the gaps between successive scans of BL 0716+714.

The data for both epochs were reduced in the Brandeis VLBI package. The polarization calibration was performed as described by Roberts, Wardle, & Brown (1994). The unpolarized sources OQ208 and 3C 84 were used to calibrate the instrumental polarizations, and observations of the compact source 0954+658 (Gabuzda et al. 1992, 1994) were used to calibrate the linear polarization position angle χ . For the 6 cm observations, the integrated polarization measurements for this calibration were provided by the VLA observations that were obtained simultaneously with the VLBI observations, and the χ calibration should be accurate to within 2–3 degrees.

In the case of the 1.3 cm/3.6 cm observations, it was not possible to obtain integrated polarization measurements at these wavelengths on the day of the experiment. We therefore had to rely on observations with the University of Michigan 26-m antenna at 3.6 cm and 2 cm and with the Effelsberg 100-m antenna at 2.8 cm and 9 mm; these sets of observations were one day before or after the VLBI observations. The Michigan and Effelsberg observations of the polarization properties of 0954+658 and BL 0716+714 are summarized in Table 1. The calibration at 3.6 cm was straightforward, since 0954+658 was detected with high signal/noise ratio, and should be accurate to within a few

degrees. The calibration at 1.3 cm was more difficult, due to the lower sensitivity of these observations. However, we believe it is accurate to within $\sim 5^\circ$, since the Effelsberg measurements at the surrounding wavelengths of 2.8 cm and 9 mm yield the same integrated χ value to within the errors (see Table 1), making it very likely that this is the integrated χ value at 1.3 cm as well. In addition, the integrated measurements from Michigan and Effelsberg yield quite consistent results. We cannot exclude the possibility that the polarization of 0954+658 varied in the time between our 1.3 cm/3.6 cm VLBI experiment and the integrated observations, however, the measurements made 1 day before and 1 day after the VLBI observations do not give any evidence for substantial variability; in addition, the absolute χ corrections implied by the integrated and milliarcsecond-scale measurements of 0954+658 and BL 0716+714 are quite consistent.

Hybrid maps of the distribution of total intensity I were made using a self-calibration algorithm similar to that described by Cornwell and Wilkinson (1981). Maps of the linear polarization¹ P were made by referencing the calibrated cross-hand fringes to the parallel-hand fringes using the antenna gains determined in the hybrid mapping, Fourier transforming the cross-hand fringes, and performing a complex CLEAN. One byproduct of this procedure is to register the I and P maps to within a small fraction of a beamwidth, so that corresponding I and P images may be directly superimposed. Model fits to the calibrated complex I and P visibilities were obtained in the Brandeis package.

The 1.3/3.6 cm VLBA data were also calibrated and imaged in AIPS using the task LPCAL (Leppänen 1995). The final I and P images obtained in the two packages were very similar, giving us confidence in the reliability of our results. We show here only the images obtained in the Brandeis package, since it is these visibility data that were used for the I and P model fitting.

¹ $P = pe^{2ix} = mIe^{2ix}$, where $p = mI$ is the polarized intensity, m is the fractional linear polarization, and χ is the position angle of the electric vector on the sky

Table 2. Source models

	I (mJy)	p (mJy)	χ_o^a (deg)	m (%)	r (mas)	Δr (mas)	PA (deg)	Δ PA (deg)	FWHM (mas)
$\lambda = 6$ cm, 1991.43									
Core	324.2	12.5	-68.5	3.3	–	–	–	–	0.25
C2	41.0	< 1	–	< 2	0.77	0.01	10	1	0.19
C1	12.2	< 1	–	< 8	2.08	0.04	12	1	0.71
$\lambda = 3.6$ cm, 1994.22									
Core	290.1	5.8	5.9	2.0	–	–	–	–	0.12
X3	17.7	< 1.5	–	< 8.5	0.67	0.01	22	2	0.28
X2	9.0	< 1.5	–	< 17	1.09	0.02	11	2	–
X1	5.5	< 1.5	–	< 27	2.31	0.04	25	1	0.28
X0A	7.4	< 1.5	–	< 20	3.35	0.06	13	1	0.82
X0A	3.2	< 1.5	–	< 47	6.06	0.30	-8	5	2.01
$\lambda = 1.3$ cm, 1994.22									
Core	265.1	9.1	2.9	3.4	–	–	–	–	0.04
K3	7.3	3.4	34.6	46.6	0.34	0.03	0	12	0.17
K2	6.5	< 3	–	< 50	0.97	0.08	24	5	0.29
K1	3.7	< 3	–	< 80	2.24	0.09	1	3	0.24

^a 6 and 3.6 cm χ values corrected for integrated rotation measure.

3. Results

In each of the images that are shown in Figs. 1–3, the restoring beams are shown as crosses in a corner of the images. For the linear polarization maps, the contours are those of polarized intensity p , and the plane of the electric vector is indicated by the polarization position angle vectors that are superimposed. The model fits for each of the calibrated visibility data sets are presented in Table 2, which gives for each component its (1) total intensity I , (2) polarized flux p , (3) polarization position angle corrected for integrated Faraday rotation χ_o , (4) degree of polarization m , (5) separation from the core r , (6) error in r , (7) structural position angle from the core PA, (8), error in PA, and (9) Gaussian size (FWHM). The positions of components from the model fitting are indicated on the I images. The errors given in this table are purely formal 1σ error estimates, based on an increase in the χ^2 for the best fit by 1.

The integrated rotation measure of BL 0716+714 is only -29 rad/m² (Rusk 1988), corresponding to rotations of 6.0, 2.2, and 0.3 degrees at 6, 3.6, and 1.3 cm, respectively. There is no evidence from our simultaneous 3.6/1.3 cm data to indicate that the rotation measure on milli-arcsecond scales is significantly different from this. We will apply the corrections implied by the integrated rotation measure to the observed VLBI χ values at 6 and 3.6 cm, and denote the resulting estimates of the intrinsic polarization position angle χ_o ; the correction for the 1.3 cm data is obviously negligible.

3.1. $\lambda = 6$ cm, 1991.43 (June 6)

The compact, one-sided core–jet structure in structural position angle $PA \sim 13^\circ$ previously observed by Eckart et al. (1987) and analyzed in that paper and by Witzel et al. (1988) is visible in our 6 cm I image (Fig. 1a). At epoch 1991.43, the structure consists of a core plus two jet components at separations ~ 0.8

(C2) and 2.1 (C1) mas from the core. The milliarcsecond-scale emission is very core-dominated: 79% of the emission on mas scales is contained in the VLBI core.

Eckart et al. (1987) observed BL 0716+714 at 6 cm at epochs 1979.93 and 1983.25. They found the source to have a double structure, with separations of 1.3 mas and 1.6 mas at the two epochs. The predicted location for the jet component detected by Eckart et al. (assuming that it continued to travel outward from the core at the speed suggested by their two epochs) at our 6 cm epoch is ~ 2.3 mas, near the separation of our jet component C1, $r = 2.08$ mas.

The only component for which polarization was detected was the VLBI core, which is polarized 3.3% with $\chi_o = -68.5^\circ$, nearly perpendicular to the jet direction (Fig. 1b).

3.2. $\lambda = 3.6$ cm, 1994.22 (March 21)

The 3.6 cm I image in Fig. 2a is the deepest of our three images. It clearly shows the jet extending nearly directly north, then possibly beginning to curve westward. It is possible that this represents the VLBI jet curving toward the arcsecond-scale structure, which lies in position angle $\sim -55^\circ$, but it may also be that this reflects local “wiggling” of the jet.

We have modelled the source structure as a core and five VLBI jet components. Here, again, the VLBI structure is extremely core-dominated, with 87% of the emission on mas scales contained in the VLBI core. It seems plausible that the component X1 detected at a separation of $r = 2.31$ mas from the core is the component C1 detected in our earlier 6 cm image, since this separation is very close to that predicted by the data at the three 6 cm epochs — $r_{C1,pred} = 2.28$ mas.

The core was polarized 2.0% in position angle $\chi_o = 6^\circ$, aligned with the jet direction (Fig. 2b).

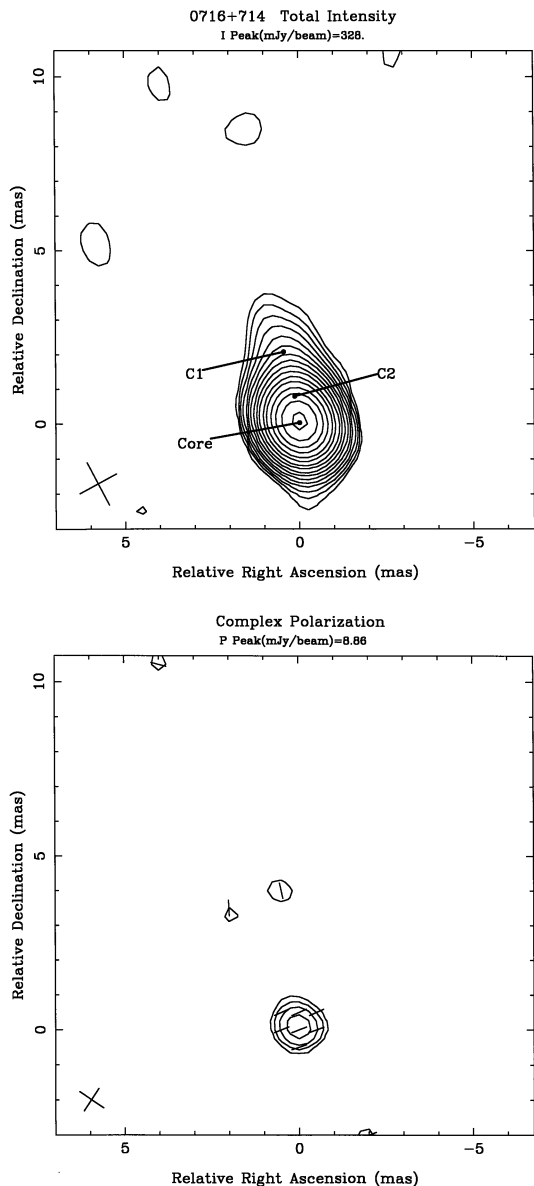


Fig. 1a and b. VLBI hybrid maps of BL 0716+714 at 6 cm, epoch 1991.43: **a** I , with contours at $-0.5, 0.5, 0.7, 1.0, 1.4, 2.0, 2.8, 4.0, 5.6, 8.0, 11.3, 16.0, 22.6, 32.0, 45.2, 64.0,$ and 90.5% of the peak brightness of 0.33 Jy/beam. **b** P , with contours of polarized intensity at $8.0, 16.0, 32.0,$ and 64.0% of the peak brightness of 8.9 mJy/beam, and χ vectors superimposed. χ has been corrected for the integrated rotation measure, which corresponds to a rotation of -6° at 6 cm.

3.3. $\lambda = 1.3$ cm, 1994.22

We have modelled the 1.3 cm source structure in Fig. 3a as a core and three jet components. In this case, 94% of the flux on mas scales is contained in the VLBI core.

These are among the very first VLBI polarization observations at 1.3 cm. The 1.3 cm core polarization was 3.4% in $\chi = 3^\circ$, roughly aligned with the jet direction (Fig. 3b). In addition, polarization was detected from the innermost 1.3 cm jet component: its degree of polarization is quite high, $\sim 47 \pm 17\%$, with χ roughly aligned with the jet direction, as would be

expected if this component were associated with a transverse shock. This high degree of polarization leaves no doubt that this emission is optically thin, and that the magnetic field is rather well ordered.

4. Discussion

4.1. Spectral indices

Our 3.6 cm and 1.3 cm images are simultaneous in time, and we can determine spectral indices for individual VLBI components that are present on both images. In the inner part of the 3.6 cm jet, there are three components that appear to correspond to the three components in the 1.3 cm jet. The separations of two of these — X1/K1 and X2/K2 — agree to within their errors, suggesting that possible frequency-dependent shifts in the VLBI core positions (Lobanov 1996) are too small to be visible in our data. We accordingly have not made any attempt to take account of this effect. It also seems natural to suggest that the innermost features X3 and K3 detected at 3.6 cm and 1.3 cm represent the same component, though in this case, the positions do not agree to within their formal error estimates. The position of the component X3 is somewhat poorly determined, however, since it is not yet well resolved from the 3.6 cm VLBI core at our observing epoch.

We have accordingly estimated spectral indices α for the core and the three jet components X1/K1, X2/K2, and X3/K3 ($F_\nu \sim \nu^\alpha$). The spectral index of the core $\alpha_{8.4-22.2}^C = -0.09 \pm 0.01$, indicating that it is predominantly optically thick, as expected. The spectral indices for the three knots in the VLBI jet are $-0.9 \pm 0.5, -0.3 \pm 0.2,$ and -0.4 ± 0.3 , from innermost knot outward. The large uncertainties in these spectral indices are due to the low fluxes of these jet components and the corresponding comparatively large uncertainties in their fluxes, especially at 1.3 cm.

4.2. VLBI core polarization

The degree of linear polarization for the VLBI core is 2–4% at all frequencies, as is typical for BL Lacertae objects at 6 cm and 3.6 cm (Gabuzda et al. 1992, 1994; Gabuzda and Cawthorne 1996). The core polarization at our earlier (6 cm) epoch was roughly perpendicular to the jet direction, $\chi_o = -68.5^\circ$. On May 21, 1991, the Effelsberg 100-m telescope measured the integrated 6 cm polarization to be in position angle $\sim 15^\circ$, showing that large swings in χ can occur on timescales of ~ 2 weeks.

At our second epoch, 1994.22, the polarization angle χ in the core was aligned with the VLBI jet direction. Measurements from the University of Michigan 26-m monitoring program indicate that this is a preferred orientation for the integrated radio polarization position angle, though large rotations in χ through 90° or more can sometimes occur on timescales as short as a few days. The two polarization position angle orientations we observed in our two VLBI epochs (parallel to and perpendicular to the VLBI jet) are those typical of the core polarizations in BL Lacertae objects (Gabuzda et al. 1994).

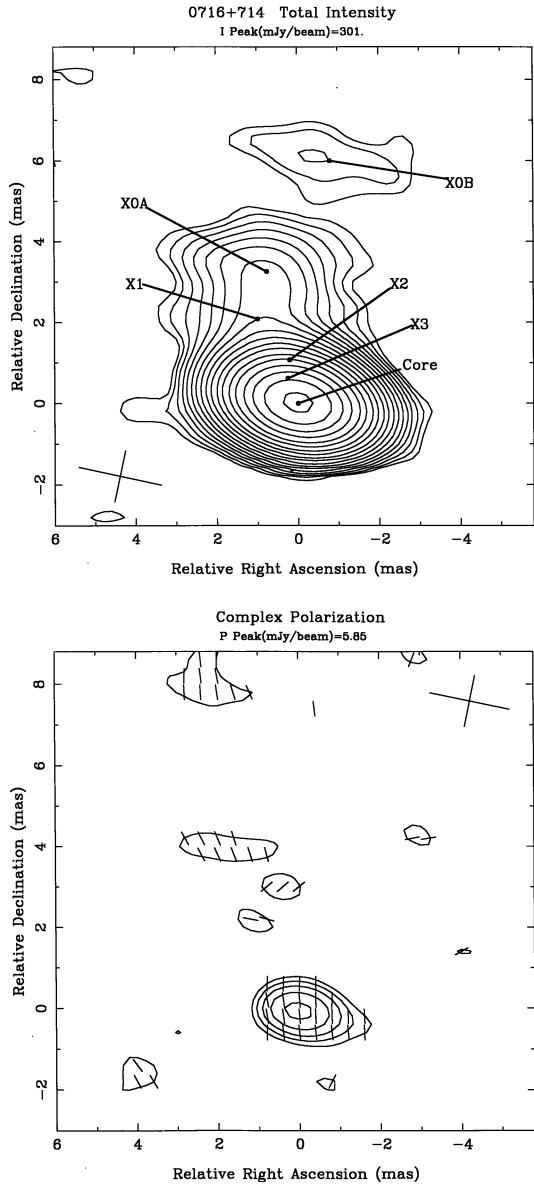


Fig. 2a and b. VLBI hybrid maps of BL 0716+714 at 3.6 cm, epoch 1994.22: **a** I , with contours at $-0.25, 0.25, 0.35, 0.5, 0.7, 1.0, 1.4, 2.0, 2.8, 4.0, 5.6, 8.0, 11.3, 16.0, 22.6, 32.0, 45.2, 64.0$, and 90.5% of the peak brightness of 0.30 Jy/beam. **b** P , with contours of polarized intensity at $22.6, 32.0, 45.2, 64.0$, and 90.5% of the peak brightness of 5.8 mJy/beam, and χ vectors superimposed. χ has been corrected for the integrated rotation measure, which corresponds to a rotation of -2.2° at 3.6 cm.

4.3. Superluminal motion in BL 0716+714 — Barely

Fig. 4 presents a plot of the separation of the 6 cm component C1 from the core as a function of time, assuming that this is the same jet component studied by Eckart et al. (1987) and Witzel et al. (1988). We have included the 3.6 cm component X1 that we believe is also likely this same component. As can be seen, the resulting four points lie very nearly on a straight line, inferring proper motion at a nearly constant speed $\sim 0.07 \pm 0.01$ mas/yr over a period of nearly fifteen years (the difference in

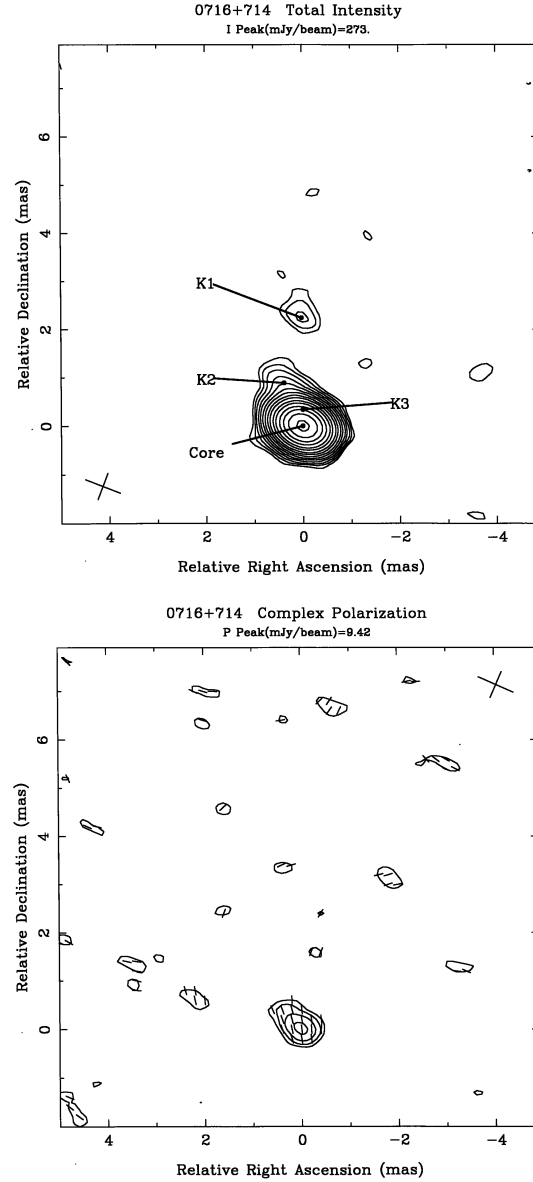


Fig. 3a and b. VLBI hybrid maps of BL 0716+714 at 1.3 cm, epoch 1994.22: **a** I , with contours at $-0.7, 0.7, 1.0, 1.4, 2.0, 2.8, 4.0, 5.6, 8.0, 11.3, 16.0, 22.6, 32.0, 45.2, 64.0$, and 90.5% of the peak brightness of 0.27 Jy/beam. **b** P , with contours of polarized intensity at $32.0, 45.2, 64.0$, and 90.5% of the peak brightness of 9.4 mJy/beam, and χ vectors superimposed.

the best fit line if we include X1 or do not include it is negligible compared to the estimated error for the speed). Again, our 6 cm and 3.6 cm images suggest that the apparent separations of components from the core do not significantly depend on the observing frequency.

It is also possible that the two features labelled C2 and X2 are the same component. If the apparent separation from the core for this component also does not depend significantly on frequency, as appears to be the case for C1/X1, its tentative two-epoch proper motion is 0.11 mas/yr. If the proper motions of VLBI components in BL 0716+714 are typically ~ 0.1 mas/yr,

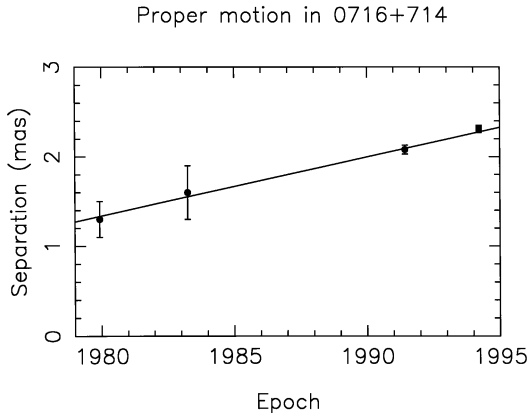


Fig. 4. Separation of the 6 cm component C1 from the core as a function of time, assuming that this is the same jet component observed by Eckart et al. (1987). The circles correspond to the three 6 cm measurements. We have also included the 3.6 cm component X1 that we believe is also likely this same component (square). The line is a least squares fit to the three 6 cm points. Including the 3.6 cm point in the fit does not significantly affect the resulting parameters for the line.

X3, which has a separation ~ 0.67 mas in our 3.6 cm image at 1994.22, would have been roughly 0.4 mas from the core at epoch 1991.43, so that it is not surprising that we did not detect this component in our 6 cm image.

If the redshift of BL 0716+714 is greater than 0.3, as argued by Wagner et al. (1996), the inferred apparent velocity for C1/X1 is $\beta_{app}h > 0.82 \pm 0.11$, well within the limit $\beta_{app}h \leq 2.3$ inferred earlier by Schalinski et al. (1992) based only on the first two epochs. The tentative apparent velocity for C2/X2 is $\beta_{app}h > 1.28$. These speeds are consistent with the evidence that the observed speeds in BL Lacertae objects are on average lower than those in quasars (Gabuzda et al. 1994).

4.4. The angle to the line of sight of the compact jet in BL 0716+714

Let us suppose that our component C2/X2 is indeed the same jet component detected by Eckart et al. (1987). One way to reconcile the large Doppler factors implied by the variability, $D \sim 10 - 20$, with the modest VLBI component velocities derived from our observations is for the angle of the jet to the line of sight θ to be significantly smaller than $1/\gamma$ — the angle at which the apparent component speed in the plane of the sky is maximized ($\gamma = 1/\sqrt{1-\beta^2}$ is the Lorentz factor of the motion). Using the usual definition of the Doppler factor $D = (\gamma(1-\beta \cos \theta))^{-1}$ to solve for $\cos \theta$ and $\sin \theta$ in terms of D , γ , and β , eliminating $\cos \theta$ and $\sin \theta$ from the usual expression for the apparent motion of a component in the plane of the sky

$$\beta_{app} = \frac{\beta \sin \theta}{1 - \beta \cos \theta} \quad (1)$$

and solving for γ , we find that (see also Roland & Hermsen 1995)

$$\gamma = \frac{\beta_{app}^2 + D^2 + 1}{2D} \quad (2)$$

Thus, if we have estimates for β_{app} and the corresponding Doppler factor D , we can estimate γ , and hence the intrinsic velocity of the motion β and the angle to the line of sight θ .

For example, if we simultaneously require $D = 10 - 20$ based on the observed variability time scales and $\beta_{app} = 0.8 - 1.3$, we find $\gamma = 5.1 - 10.1$, $\beta = 0.980 - 0.995$, and $\theta = 0.2 - 1.5^\circ$. The angle at which the apparent component speed would be maximized is $\theta_0 = 1/\gamma \sim 6 - 11^\circ$. We see that the effect of simultaneously requiring large Doppler factors and small apparent speeds has been to bring θ substantially closer to the line of sight. Thus, if the Doppler factors for the regions of rapid variability are essentially the same as those for the moving components whose speeds we have estimated, very small angles to the line of sight are required.

We can also use the observed degree of polarization of K3 to put limits on the line of sight of the jet (Cawthorne & Wardle 1988). Essentially, if we assume this component is a shock, the measured degree of polarization constrains the angle ϵ between the line of sight and the jet in the source (shock) frame. The maximum value for ϵ corresponds to the maximum compression for the shock; for $m = 0.47$, $\epsilon_{max} \sim 29^\circ$. We could relate this to the angle of the jet to the line of sight in the observer's frame, θ , and to γ if we knew the apparent velocity of this component β_{app} (Cawthorne & Wardle 1988). Although we do not have any velocity measurements for K3, it is interesting to see what values are implied for γ and θ if we assume that the proper motion for K3 is similar to that for the other components for which we have measurements $\mu \sim 0.1$ mas/yr. In this case, we find that if $z = 0.3$, $\gamma = 1.53 - 1.65$, $22^\circ < \theta < 59^\circ$, and the maximum possible Doppler factor (which corresponds to the minimum angle to the line of sight) is $D_{max} = 2.3$. Even if the redshift is as large as $z \sim 1.0$ (roughly the maximum redshift measured for any BL Lacertae object in the complete 1 Jy sample defined by Kühr and Schmidt (1990), which includes BL 0716+714), we find $\gamma = 2.95 - 3.32$, $10^\circ < \theta < 29^\circ$, and $D_{max} = 4.8$. Thus, this analysis indicates that the observed polarization of K3 is inconsistent with angles to the line of sight as small as those inferred by the Doppler factors implied by the rapid variability.

Thus, it is difficult to directly reconcile the rather large Doppler factors implied by the rapid variability, the modest apparent VLBI component speeds, and the constraints derived from the high polarization of K3. One possibility is that the Doppler factors for the measured VLBI components are substantially lower than the value $D = 10 - 20$ suggested by the variability timescales. For example, it may be that the region giving rise to the rapid variability is on more compact scales than those probed by our VLBI measurements, and that the jet either significantly decelerates or experiences a substantial bend away from the line of sight by the time it reaches the scales in our images. It is also possible that the pattern speed of the shock associated with K3 differs appreciably from the flow speed, and/or that this shock is oblique; however theoretical shock pattern speeds are typically not more than two or three times higher or lower than the speed of the underlying flow, so

that it is difficult to fully reconcile the inferred large Doppler factors and modest VLBI component speeds in this way.

5. Conclusion

The images presented here indicate that BL 0716+714 displays a number of properties that are characteristic of BL Lacertae objects. The core polarization for all three frequencies was $\sim 2\text{--}4\%$. The polarization position angle χ in the core was roughly perpendicular to the VLBI jet direction $PA \sim 13^\circ$ at our first epoch (6 cm, 1991.43), but aligned with PA at our second epoch (3.6 cm and 1.3 cm, 1994.22). The only jet component in which polarization was detected was K3, at 1.3 cm, in which χ was aligned with the jet direction. The degree of polarization is quite high, $47 \pm 17\%$, demonstrating that this component is optically thin and that the magnetic field must be rather well-ordered. Since the emission is optically thin, the inferred magnetic field is transverse to the jet direction.

We have identified a VLBI component that has apparently moved at a constant speed of 0.07 ± 0.01 mas/yr over a period of nearly fifteen years. We have identified a second moving component based on our two epochs of data, whose tentative two-epoch proper motion is similar — ~ 0.11 mas/yr. If the redshift of BL 0716+714 is $z > 0.3$, as suggested by Wagner et al. (1996), these proper motions correspond to apparent speeds of $\beta_{app}h > 0.82 \pm 0.11$ and $\beta_{app}h > 1.28$. These speeds are consistent with previous results that show BL Lacertae objects to have more modest VLBI component speeds than quasars (Gabuzda et al. 1994), typically $\beta_{app}h \sim 1 - 4$. If the redshift for BL 0716+714 proves to be $z < 0.39$, the apparent motion in component C1/X1 will be subluminal, making BL 0716+714 one of only two BL Lacertae objects known to have subluminal speeds. BL 0716+714 especially stands out in this regard, since the other subluminal source, 1652+398, may well be more appropriately classified as a radio galaxy than a true BL Lacertae object (Gabuzda et al. 1992).

Since BL 0716+714 is rather core-dominated, it is tempting to think that, at least on some scales, its jet is viewed at angles to the line of sight less than the angle that maximizes the observed velocity, $1/\gamma$. In this picture, we would expect the core emission to be very highly beamed, which would be consistent with the rapid variability observed in BL 0716+714. It is difficult to reconcile the large Doppler factors required by the rapid variability with the moderate VLBI component velocities in BL 0716+714, however. One plausible explanation for this contradiction is that the rapid variability occurs on more compact scales than those imaged by our VLB array, and that the jet decelerates and/or bends by the time it gets to the scales in our images.

Acknowledgements. We thank U. Stursberg and H. Blaschke for their efforts at the MkIII correlator of the MPIfR (Bonn) and M. Titus at the MkIII correlator at Haystack Observatory. We would also like to thank the Joint Institute for VLBI in Europe for hospitality during a visit by TPK, and K. Leppänen for his help with the data reduction in AIPS. The work of TPK was supported in part from a grant of the BMBF (Verbundforschung). This research has made use of data from the University of Michigan Radio Astronomy Observatory, which is

supported by the National Science Foundation and by funds from the University of Michigan. The VLBA is a facility of the NRAO, which is operated by Associated Universities Inc., under cooperative agreement with the NSF.

References

- Angel, J. R. P. & Stockman, H. S. 1980, *ARA&A*, 8, 321.
 Cornwell, T. J. & Wilkinson, P. N. 1981, *MNRAS*, 196, 1067.
 Cawthorne, T.V. & Wardle, J.F.C. 1988, *ApJ*, 332, 696.
 Eckart, A., Witzel, A., Biermann, P., Johnston, K. J., Simon, R., Schalinski, C., and Kühr, H. 1987, *A&AS*, 67, 121.
 Gabuzda, D. C. & Cawthorne, T. V. 1996, *MNRAS*, 283, 759.
 Gabuzda, D. C., Cawthorne, T. V., Roberts, D. H., & Wardle, J. F. C. 1992, *ApJ*, 388, 40.
 Gabuzda, D. C., Mullan, C. M., Cawthorne, T. V., Wardle, J. F. C., & Roberts, D. H. 1994, *ApJ*, 435, 140.
 Heeschen, D. S., Krichbaum, T., Schalinski, C. J., & Witzel, A. 1987, *AJ*, 94, 1493.
 Hughes, P. A., Aller, H. D., & Aller, M. F. 1989, *ApJ*, 341, 68.
 Kollgaard, R. I. 1994, *Vistas in Astronomy*, 38, 29.
 Laing, R. 1980, *MNRAS*, 193, 439.
 Lobanov, A.P. 1996, *Ph.D. Thesis*, New Mexico Institute of Mining & Technology.
 Perley, R. 1982, *AJ*, 87, 859.
 Quirrenbach, A., Witzel, A., Wagner, S., Sanchez-Pons, F., Krichbaum, T. P., Wegner, R., Anton, K., Erkens, U., Haehnel, M., Zensus, J. A., & Johnston, K. J. 1991, *ApJ*, 372, L71.
 Roberts, D. H., Wardle, J. F. C., & Brown, L. F. 1994, *AJ*, 427, 718.
 Roland, J. & Hermsen, W. 1995, *A&A*, 297, L9.
 Rusk, R. 1988, Ph.D. thesis, University of Toronto.
 Schalinski, C. J., Witzel, A., Krichbaum, T. P., Hummel, C. A., Quirrenbach, A., and Johnston, K. J. 1992, *Variability in Blazars*, E. Valtaoja & M. Valtonen, Eds. (Cambridge: Cambridge University Press), p. 225.
 Wagner, S.J., Witzel, A., Heidt, J., Krichbaum, T.P., Qian, S.J., Quirrenbach, A., Wegner, R., Aller, H., Aller, M., Anton, K., Appenzeller, I., Eckart, A., Kraus, A., Naundorf, C., Kneer, R., Steffen, W., & Zensus, J.A. 1996, *AJ*, 111, 2187.
 Witzel, A., Schalinski, C. J., Johnston, K. J., Biermann, P. L., Krichbaum, T. P., Hummel, C. A., & Eckart, A. 1988, *A&A*, 206, 245.